Retinal ganglion cell topography in patients with visual pathway pathology

Zehnder, Simon ; Wildberger, Hannes ; Hanson, James V M ; Lukas, Sebastian ; Pelz, Stefan ; Landau, Klara ; Wichmann, Werner ; Gerth-Kahlert, Christina

Abstract: BACKGROUND: To investigate and quantify the impact of intracranial lesions at different locations within the visual pathway on the ganglion cell layer-inner plexiform layer (GCL-IPL) complex and the retinal nerve fiber layer (RNFL). METHODS: Patients with intracranial lesions affecting the optic chiasm (Group I) or the optic tract and/or lateral geniculate nucleus (Group II) were included. All patients received kinetic visual field assessment and underwent spectral domain optical coherence tomography. Peripapillary and papillomacular bundle (PMB) RNFL and macular GCL-IPL thickness in 4 perifoveal areas were measured and compared with normal values derived from 52 age-matched healthy control subjects. Z-scores for each parameter of every patient were calculated and compared with the normative data. Z-scores less than -2.0 (e.g., -2.5) were considered as being statistically significant. RESULTS: Twenty-two patients (Group I and II: 13 and 9, respectively) were included. Ten of 13 patients in Group I showed significant binasal GCL-IPL thinning, with associated temporal sector thinning in 8 patients. In Group II, all 9 patients showed significant reduction of the GCL-IPL corresponding to the homonymous visual field defect, but only 4 demonstrated RNFL thinning. Contralateral RNFL thinning within the PMB clinically similar to bow-tie atrophy was evident in all patients in Group II. GCL-IPL and RNFL thinning varied in severity from mild (isolated PMB RNFL thickness reduction) to severe (bilateral asymmetrical reduction of PMB RNFL associated with asymmetric, predominantly nasal reduction of GCL-IPL) in Group I. CONCLUSION: Clinical abnormalities in patients with visual pathway lesions are more likely to demonstrate abnormalities of GCL-IPL than global peripapillary RNFL thickness. However, PMB thickness measurement appears to be a valuable tool to detect abnormalities of the anterior visual pathways. If peripapillary RNFL measurements are performed in such patients, PMB thickness should be considered the most useful quantitative parameter.

DOI: https://doi.org/10.1097/WNO.0000000000000589

Retinal Ganglion Cell Topography in Patients With Visual Pathway Pathology

Simon Zehnder, MD, Hannes Wildberger, MD, James V. M. Hanson, PhD, Sebastian Lukas, Dipl-Ing (FH), Stefan Pelz, MD, Klara Landau, MD, Werner Wichmann, MD, Christina Gerth-Kahlert, MD

Background: To investigate and quantify the impact of intracranial lesions at different locations within the visual pathway on the ganglion cell layer–inner plexiform layer (GCL–IPL) complex and the retinal nerve fiber layer (RNFL).
Methods: Patients with intracranial lesions affecting the optic chiasm (Group I) or the optic tract and/or lateral geniculate nucleus (Group II) were included. All patients received kinetic visual field assessment and underwent spectral domain optical coherence tomography. Peripapillary and papillomacular bundle (PMB) RNFL and macular GCL–IPL thickness in 4 perifoveal areas were measured and compared with normal values derived from 52 age-matched healthy control subjects. Z-scores for each parameter of every patient were calculated and compared with the normative data. Z-scores less than −2.0 (e.g., −2.5) were considered as being statistically significant.
Results: Twenty-two patients (Group I and II: 13 and 9, respectively) were included. Ten of 13 patients in Group I showed significant binasal GCL–IPL thinning, with associated temporal sector thinning in 8 patients. In Group II, all 9 patients showed significant reduction of the GCL–IPL corresponding to the homonymous visual field defect, but only 4 demonstrated RNFL thinning. Contralateral RNFL thinning within the PMB clinically similar to bow-tie atrophy was evident in all patients in Group II. GCL–IPL and RNFL thinning varied in severity from mild (isolated PMB RNFL thickness reduction) to severe (bilateral asymmetrical reduction of PMB RNFL associated with asymmetric, predominantly nasal reduction of GCL–IPL) in Group I.
Conclusion: Clinical abnormalities in patients with visual pathway lesions are more likely to demonstrate abnormalities of GCL–IPL than global peripapillary RNFL thickness. However, PMB thickness measurement appears to be a valuable tool to detect abnormalities of the anterior visual pathways. If peripapillary RNFL measurements are performed in such patients, PMB thickness should be considered the most useful quantitative parameter.

Journal of Neuro-Ophthalmology 2017;0:1–7
doi: 10.1097/WNO.0000000000000589

Retrograde trans-synaptic degeneration in primates was first described by van Buren (1), who observed reduced ganglion cell layer (GCL) thickness in the corresponding retinal areas after a lesion in the optic chiasm or after right occipital lobectomy. The severity of GCL atrophy was shown to depend on the age, extent of the lesion, and the time elapsed since the damage (2). In humans, Hoyt et al (3) applied the term homonymous hemioptic hypoplasia in describing the characteristic retinal nerve fiber layer (RNFL) atrophy and optic nerve head appearance in 3 patients with congenital cerebral hemispheric damage. The development of high-resolution optical coherence tomography (OCT) and the availability of software tools to delineate the boundaries of all retinal layers (segmentation) now allows in vivo measurements of retinal structure. Thinning of the specific RNFL sectors or the GCL–inner plexiform layer (GCL–IPL) complex in the corresponding retinal areas in patients with retrogeniculate lesions has been reported (4–10). An absence of visible MRI abnormalities in the lateral geniculate nucleus (LGN) and surrounding region does not definitively exclude damage, but may reflect the small size of the LGN or an insufficiently detailed MRI protocol.

Department of Ophthalmology (SZ, HW, JVMH, SP, KL, CG-K), Neuroimmunology and Multiple Sclerosis Research (JVMH, SL), Department of Neurology, and Department of Neuroradiology (WW), University of Zurich and University Hospital Zurich, Zurich, Switzerland.

J. V. M. Hanson is partially funded by the Clinical Research Priority Program of the University of Zurich and has received speaker fees and travel support from Biogen. S. Lukas is currently employed by Heidelberg Engineering but was employed by the University of Zurich during the study. The remaining authors report no conflicts of interest.

Supplemental digital content is available for this article. Direct URL citations appear in the printed text and are provided in the full text and PDF versions of this article on the journal's Web site (www.jneuro-ophthalmology.com).

Address correspondence to Christina Gerth-Kahlert, MD, Department of Ophthalmology, University Hospital Zurich, Frauenklinikstrasse 24, CH-8091 Zurich, Switzerland; E-mail: christina.gerth-kahlert@usz.ch

The purpose of our study was to quantify the GCL–IPL thickness in patients with anterior visual pathway pathology. It is unclear whether a reduction in RNFL thickness occurs concurrently with a thinning of the GCL–IPL. Therefore, the secondary aim of the study was to compare reductions in GCL–IPL with changes in peripapillary RNFL thickness.

METHODS

Patients

Patients were recruited from the Department of Ophthalmology of the University Hospital Zurich between May 2014 and December 2015. Inclusion criteria were as follows: a brain disorder (tumoral, ischemic, inflammatory unrelated to multiple sclerosis, or other neuroimmunological disease) affecting the intracerebral portion of the anterior visual pathway (optic chiasm, optic tract, and/or the LGN); diagnosis at least 2 months before study enrollment; brain MRI at initial evaluation; presence of visual field defects; age between 18 and 60 years.

All MRIs were re-evaluated by a neuroradiologist (W.W.) and neuro-ophthalmologist (H.W.). Patients with a lesion localized to the optic nerve without extension to the chiasm and isolated retrogeniculate lesions were excluded from the study. Other exclusion criteria were as follows: pre-existing neurological or neuroimmunological disease (such as multiple sclerosis), optic disc anomalies; pre-existing optic neuropathy; and glaucoma. Patients with nystagmus were excluded to ensure high quality of OCTs.

All patients received a comprehensive eye examination. Kinetic visual fields were manually performed by an experienced perimetrist using the Octopus 900 perimeter (Haag Streit AG, Koeniz, Switzerland). One patient with acromegaly had to be tested with the kinetic perimeter because his increased head size precluded examination with the Octopus system.

After receiving an explanation about the aims and methods of the study, every subject signed an informed consent form. The study was approved by the local Ethics committee of the Canton of Zurich and performed according to the Tenets of the Declaration of Helsinki.

Spectral Domain Optical Coherence Tomography

All spectral domain OCT (SD-OCT) measurements were obtained with Spectralis SD-OCT (software version 6.0.13.0; Heidelberg Engineering, Heidelberg, Germany). To measure the peripapillary RNFL thickness, a circular scan with a diameter of 3.5 mm centred on the optic disc was obtained. The scanned area was divided into 7 sectors as implemented in Spectralis software: nasal, temporal, nasal/temporal superior and inferior, respectively, and the papillomacular bundle (PMB) in a 30°-sector with a mild tilt of 7° downward in the temporal area (n-site PMB-program). All sectors were analyzed, along with the average (global) RNFL thickness (Fig. 1A). The macular OCT was obtained using a horizontal line scan protocol with 31 horizontal B scans, each 8-mm long and separated by 240 μm. All macular scans were automatically segmented using supplied proprietary software (version 6.0.14.0; Heidelberg Engineering).

GCL–IPL thickness was analyzed separately corresponding to the RNFL distribution in the superotemporal, superonasal, inferonasal, and inferotemporal retina. The macular area within the inner Early Treatment Diabetic Retinopathy Study (ETDRS) ring was divided into 16 quadrants centred on the fovea (Figs. 1B and 1C). The 4 innermost quadrants were excluded because of the physiological absence of ganglion cells within 63 μm of the foveal center (11). The area

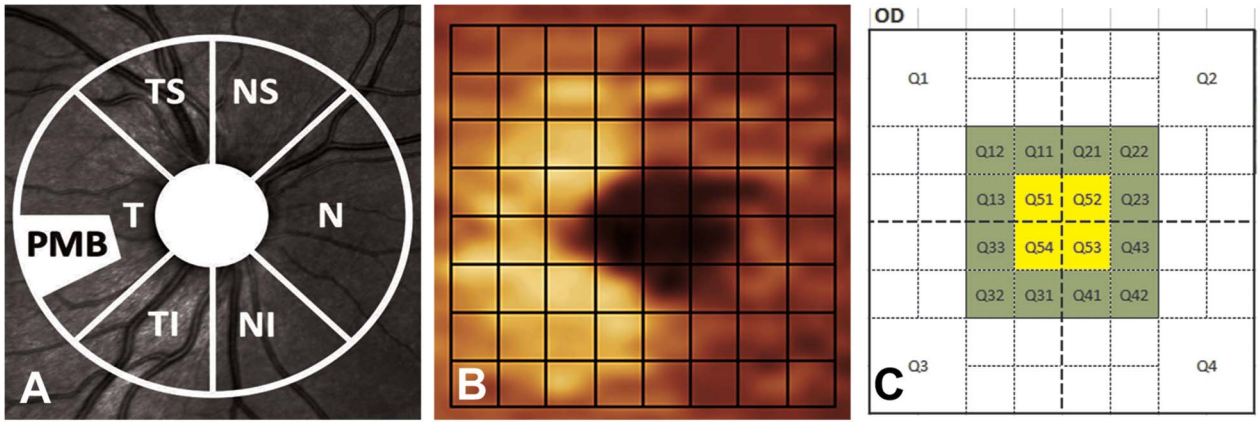

FIG. 1. A. Peripapillary RNFL schematic of the 6 sectors and the papillomacular bundle. **B.** Illustration of the analyzed macular area superimposed on a red-free fundus photograph on which was overlaid an 8 × 8 grid pattern. **C.** The areas marked in green in a right eye were used for the GCL–IPL thickness analysis. PMB, papillomacular bundle; T, temporal; TS, temporal-superior; NS, nasal-superior; N, nasal; NI, nasal-inferior; TI, temporal-inferior; T, temporal; RNFL, retinal nerve fiber layer; GCL–IPL, ganglion cell layer–inner plexiform layer; OD, right eye.

of the remaining 12 quadrants formed a right-angled pattern in each of the 4 sectors. Thus, 2 superior and inferior patterns on the nasal and temporal retina of each eye separated by a virtual vertical line through the foveola were analyzed for GCL–IPL thickness. Figure 1C depicts the analyzed retinal areas (green quadrants). The boundaries of the retinal layers as defined by the software segmentation algorithm were manually verified and, if necessary, corrected by a single operator (SZ). Mean values of GCL–IPL for every sector were calculated.

Data were compared with those derived from 52 normal subjects aged 20–60-years old. Individuals with a refractive error greater than −6.00 or +4.00 diopters (spherical equivalent), current or previously treated amblyopia, or any eye disease or anatomical abnormality, which could affect optic nerve or retinal structure or integrity, were excluded in the control group. Segmentation software defined the mean thickness of both GCL and IPL in every quadrant, which was aggregated to give corresponding values for GCL–IPL.

Statistical Analysis

We performed statistical analysis using SPSS (version 22, 2013; IBM Corp., Armonk, NY). Z-scores of both RNFL and GCL–IPL were calculated to compare patient data with those derived from the control subjects. We defined a z-score less than −2.0 as statistically significant, whereas a z-score between −1.5 and −2 was considered a trend. Cohen's kappa was calculated based on the abnormal z-scores to quantify the agreement between the measurements of GCL–IPL and RNFL thickness.

RESULTS

Twenty-two patients (16 men, 6 women) aged 20–59 years (mean 40.0 years) were included. Patients were divided into 2 groups according to the location of the intracranial lesion: Group I: lesion of the optic chiasm (13/22) and Group II: lesion involving the optic tract and/or the LGN (9/22) (see **Supplemental Digital Content**, Table E1, http://links.lww.com/WNO/A274).

Ganglion Cell Layer–Inner Plexiform Layer Analysis

In Group I, most patients (10/13; Patients 3 and 5–13) with chiasmal lesions showed significant thinning of the GCL–IPL complex binasally. This nasal thinning was associated with a thinning in one of the temporal sectors in 8 patients (Patients 3, 5–10, and 13). One patient revealed significant unilateral thinning of the nasal GCL–IPL (Patient 4).

All patients in Group II showed significant homonymous thinning of the corresponding halves or quadrants of the retina (lower z-scores were calculated for the ipsilateral temporal and contralateral nasal retinal sectors).

Retinal Nerve Fiber Layer Analysis

Patients in Group I showed a significant global RNFL thinning in both eyes (7/13; Patients 3, 5–8, 10, and 11) or 1 eye (4/13; Patients 1, 9, 12, and 13). PMB was significantly thinned in 20 of 26 eyes. Global RNFL thinning was always associated with a significant reduction within the PMB. Isolated unilateral RNFL thickness reduction within the PMB was present in 1 patient (Patient 4).

Significant bilateral thinning of global RNFL thickness was found in 4 patients in Group II (Patients 14, 18, 19, and 22). All patients demonstrated a significant (8/9; Patients 14, 15, and 17–22) or almost significant (1/9; z-score −1.76, Patient 16) RNFL reduction within the PMB. PMB was affected in the eye contralateral to the lesion in 8 patients and bilaterally in1 patient (Patient 18). All RNFL data are plotted together with the GCL-IPL analysis and visual fields in Figures 2 and 3.

Comparison between Ganglion Cell Layer–Inner Plexiform Layer and Retinal Nerve Fiber Layer

Overall, OCT analysis demonstrated a significant reduction of global RNFL thickness in 15/22 patients, whereas GCL–IPL thickness was reduced in 20/22 patients.

Comparison between PMB RNFL and GCL–IPL in Group I revealed, as expected, retinal damage that varied in severity and extent. No significant change in RNFL or GCL–IPL was evident in Patient 2, despite the chiasmal lesion. Reduction of PMB RNFL without significant GCL–IPL changes was seen in 1 patient (Patient 1). A reduction of PMB RNFL associated with nasally reduced GCL–IPL in the same eye was visible in Patient 4. More significant damage, with reduced PMB RNFL in 1 eye associated with symmetrical or asymmetrical nasal reduction of GCL-IPL in both eyes, was recorded in 2 patients (Patients 3 and 12). The most advanced damage in Group I was evident in 8 patients with bilateral asymmetrical reduction of PMB RNFL associated with asymmetrical (with a nasal predilection) thinning of GCL–IPL (Patients 5, 6, 7, 8, 9, 10, 11, and 13).

Reduced RNFL within the PMB contralateral to the lesion was associated with GCL–IPL thinning in the lesion-corresponding area in all except 1 patient (Patient 16) in Group II.

Cohen's kappa calculated for the 2 methods (GCL–IPL and global RNFL thickness) was 0.207 showing some degree of agreement between GCL–IPL and global RNFL in the detection of reterograde degeneration. However, this did not reach statistical significance ($P = 0.059$). Agreement between PMB and GCL-IPL was strong at 0.553 ($P < 0.001$). GCL–IPL analysis better reflected the relationship between the site of damage, secondary retinal atrophy, and corresponding visual field defect. By contrast, RNFL thickness was reduced, but it remains challenging to reconcile the recorded visual field defects

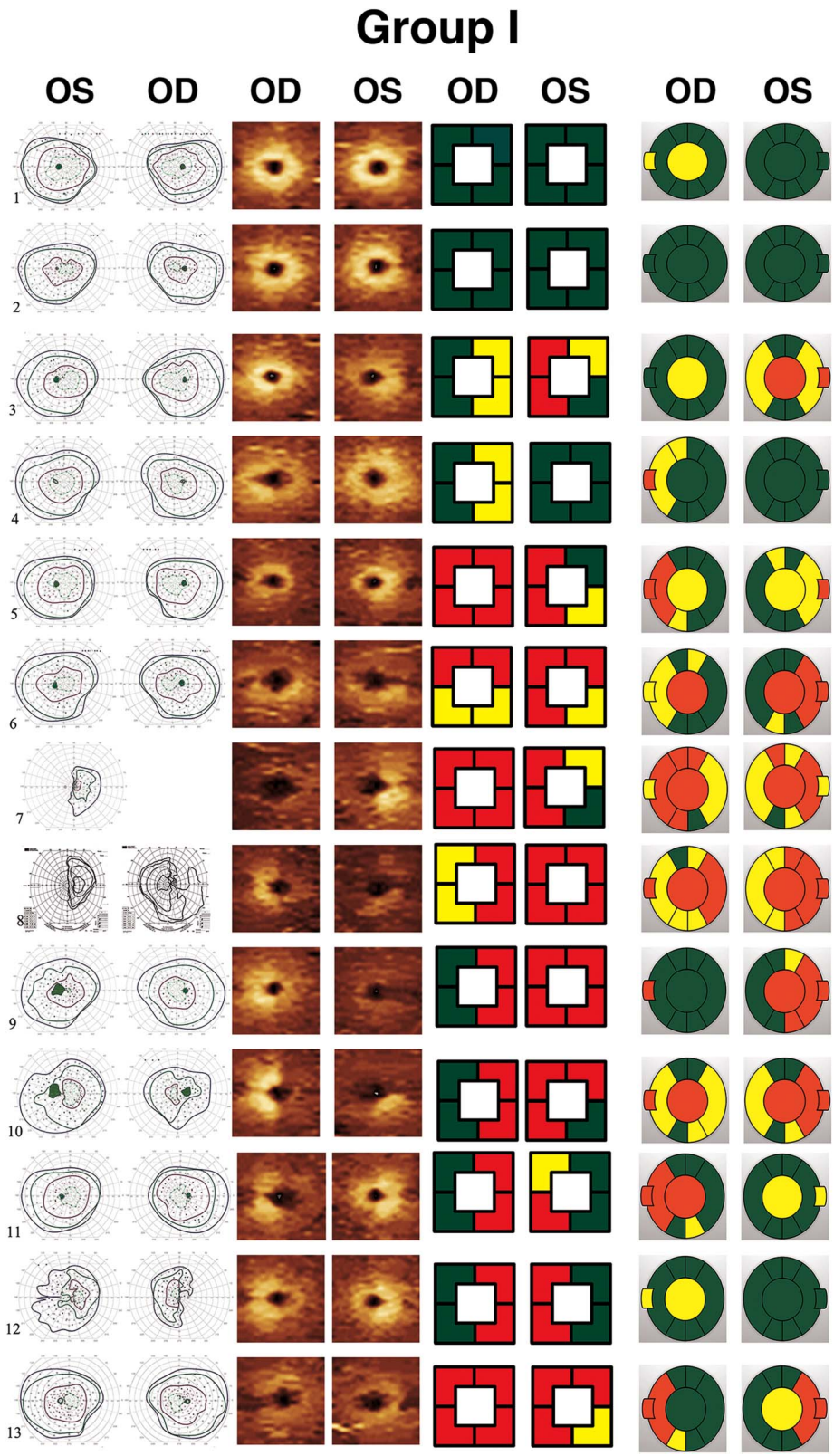

FIG. 2. Kinetic visual fields, GCL–IPL thickness profile, GCL–IPL thickness z-scores of the 4 quadrants and peripapillary RNFL thickness map including the PMB area (from left to right) are shown in 4 adjacent columns for both eyes of each patient. Z-scores: Normal (>−2.0, green), significantly reduced (−2 to −3, yellow), severely reduced (<−3, red). GCL–IPL, ganglion cell layer–inner plexiform layer; RNFL, retinal nerve fiber layer; OD, right eye; PMB, papillomacular bundle; OS, left eye; V4e, blue; I4e, green; I2e, brown/purple; I1e, light green.

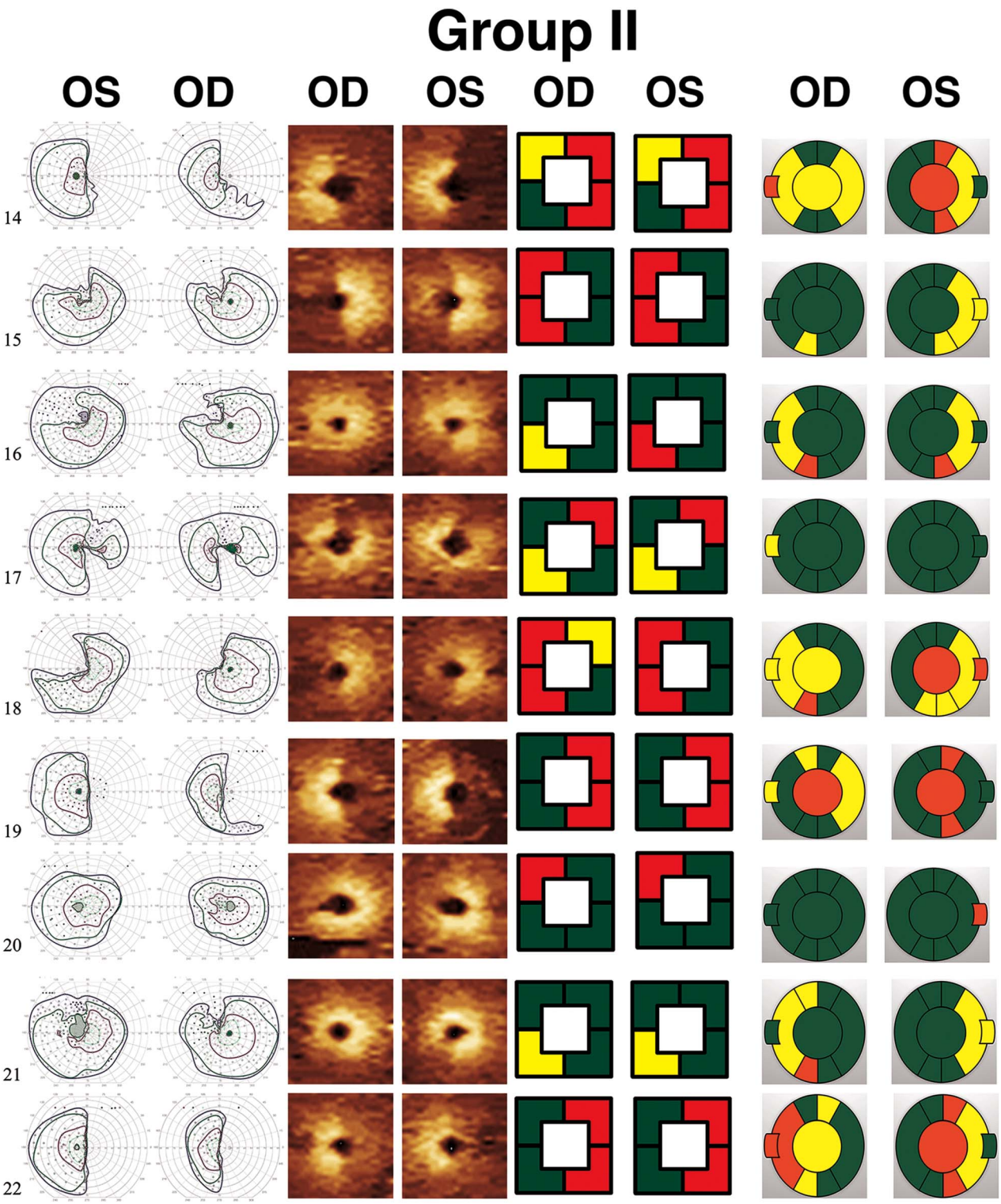

FIG. 3. Kinetic visual fields, GCL–IPL thickness profile, GCL–IPL thickness z-scores of the 4 quadrants and peripapillary RNFL thickness map including the PMB area (from left to right) are shown in 4 adjacent columns for both eyes of each patient. Z-scores: Normal (>−2.0, green), significantly reduced (−2 to −3, yellow), severely reduced (<−3, red). GCL–IPL, ganglion cell layer–inner plexiform layer; RNFL, retinal nerve fiber layer; OD, right eye; PMB, papillomacular bundle; OS, left eye; V4e, blue; I4e, green; I2e, brown/purple; I1e, light green.

with patterns of RNFL structural loss in cases of mixed LGN and chiasmal pathology. A specific and pathognomonic RNFL thickness change is observable in lesions of the LGN; the severity of damage may modify the extent of the visual field defect. An example is seen in Figure 3, Patient 14 with right homonymous visual field defect. Despite the homonymous GCL hemiatrophy, RNFL atrophy of the temporal arcuate bundles with a normal thickness within the PMB was observed in the left eye ipsilateral to the affected LGN. However, the contralateral eye revealed a bow-tie optic atrophy with reduced RNFL thickness within the PMB.

DISCUSSION

The probable degeneration pattern of RNFL or GCL-IPL as revealed by OCT segmentation after damage to the anterior visual pathway has been the subject of previous research (4–10,12–16). A lesion localized anteriorly between the LGN and optic nerves is characterized by a retrograde (descending) axonal degeneration, in contrast to anterograde (ascending) Wallerian degeneration.

Our microstructural retinal analysis in patients with lesions of the anterior visual pathway at different sites showed a reduction in the thickness of the ganglion cells and their axons corresponding to the lesion site. In contrast to previous studies, we investigated patients with lesions of the intracerebral portion of the anterior visual pathways. Patients with chiasmal lesions displayed variable GCL–IPL and RNFL damage, from minimal to severe thinning. Most patients with chiasmal lesions showed a binasal thinning of the GCL–IPL complex as reported by Tieger et al (17). The reduction was not strictly symmetrical and was associated with thinning of the temporal GCL–IPL in most cases. This asymmetry may be due to the variable effects of tumors compressing crossing and noncrossing fibers within the optic chiasm (18).

Retrograde homonymous hemiretinal degeneration was evident in all patients with a lesion involving the LGN (Group II). Our clinical experience of such cases would suggest that the resulting visual field defects were most likely permanent, whereas such defects tended to improve in patients with chiasmal lesions after decompression. Group I patients showed visual field recovery in the presence of substantial retinal neural and axonal damage. Therefore, quantification of the retinal layers should always be performed in patients with chiasmal lesions, even those with improving or absent visual field defects. Quantification of GCL–IPL will be required as part of the clinical assessment of patients to improve counseling and to define the endpoint of visual field loss. Our GCL–IPL thickness analysis based on 4 right angle–shaped sectors covering the portion of the macula with the thickest GCL provides a useful investigative tool. Overall, our results are supportive of those reported by Akashi et al (19). However, in that study, only patients with chiasmal lenses were included, and there was no analysis of PMB thickness. RNFL thickness measurements (with the exception of PMB) are of less clinical utility than those of GCL–IPL.

Our RNFL analysis highlights the importance of the isolated PMB measurement. Despite the small number of patients studied and absence of retrogeniculate lesions, we can conclude that thinning of the PMB is a more accurate predictor of retrograde degeneration than abnormal global or sectorial RNFL thickness. Unfortunately, PMB measurements are not currently implemented in all OCT devices. The bilateral automated segmentation in 4 retinal sectors within the inner ETDRS ring described here provided useful information regarding potential atrophy of the inner retina. Careful manual verification and correction of the automated segmentation is essential.

Our results emphasize the necessity of careful and detailed RNFL thickness evaluation in patients with visual pathway pathology. Further investigations, in particular in patients with retrogeniculate lesions, are recommended to determine the degenerative process in the GCL and RNFL. In addition, the use of high-field MRI with increased spatial resolution to visualize the LGN will permit a better correlation of intracerebral and retinal layer morphology.

ACKNOWLEDGMENTS

Biostatistics support by Burkhardt Seifert, PhD at the Epidemiology, Biostatistics and Prevention Institute, University of Zurich, Zurich.

REFERENCES

1. **Van Buren JM**. Trans-synaptic retrograde degeneration in the visual system of primates. J Neurol Neurosurg Psychiatry. 1963;26:402–409.
2. **Hendrickson A**, Warner CE, Possin D, Huang J, Kwan WC, Bourne JA. Retrograde transneuronal degeneration in the retina and lateral geniculate nucleus of the V1-lesioned marmoset monkey. Brain Struct Funct. 2015;220:351–360.
3. **Hoyt WF**, Rios-Montenegro EN, Behrens MM, Eckelhoff RJ. Homonymous hemioptic hypoplasia. Fundoscopic features in standard and red-free illumination in three patients with congenital hemiplegia. Br J Ophthalmol. 1972;56:537–545.
4. **Keller J**, Sanchez-Dalmau BF, Villoslada P. Lesions in the posterior visual pathway promote trans-synaptic degeneration of retinal ganglion cells. PLoS One. 2014;9:e97444.
5. **Jindahra P**, Petrie A, Plant GT. The time course of retrograde trans-synaptic degeneration following occipital lobe damage in humans. Brain. 2012;135:534–541.
6. **Jindahra P**, Petrie A, Plant GT. Retrograde trans-synaptic retinal ganglion cell loss identified by optical coherence tomography. Brain. 2009;132:628–634.
7. **Mitchell JR**, Oliveira C, Tsiouris AJ, Dinkin MJ. Corresponding ganglion cell atrophy in patients with postgeniculate homonymous visual field loss. J Neuroophthalmol. 2015;35:353–359.
8. **Meier PG**, Maeder P, Kardon RH, Borruat FX. Homonymous ganglion cell layer thinning after isolated occipital lesion: macular OCT demonstrates transsynaptic retrograde

retinal degeneration. J Neuroophthalmol. 2015;35:112–116.
9. **Meier P**, Maeder P, Borruat FX. Transsynaptic retrograde degeneration: clinical evidence with homonymous RGCL loss on OCT. Klin Monbl Augenheilkd. 2016;233:396–398.
10. **Mehta JS**, Plant GT. Optical coherence tomography (OCT) findings in congenital/long-standing homonymous hemianopia. Am J Ophthalmol. 2005;140:727–729.
11. **Curcio CA**, Allen KA. Topography of ganglion cells in human retina. J Comp Neurol. 1990;300:5–25.
12. **Yamashita T**, Miki A, Iguchi Y, Kimura K, Maeda F, Kiryu J. Reduced retinal ganglion cell complex thickness in patients with posterior cerebral artery infarction detected using spectral-domain optical coherence tomography. Jpn J Ophthalmol. 2012;56:502–510.
13. **Moon H**, Yoon JJ, Lim HT, Sung KR. Ganglion cell and inner plexiform layer thickness determined by spectral domain optical coherence tomography in patients with brain lesions. Br J Ophthalmol. 2015;99:329–335.
14. **Goto K**, Miki A, Yamashita T, Araki S, Takizawa G, Nakagawa M, Ieki Y, Kiryu J. Sectoral analysis of the retinal nerve fiber layer thinning and its association with visual field loss in homonymous hemianopia caused by post-geniculate lesions using spectral-domain optical coherence tomography. Graefes Arch Clin Exp Ophthalmol. 2016;254:745–756.
15. **Lloyd-Smith AJ**, Narayana K, Warren F, Balcer LJ, Galetta SL, Rucker JC. Optical choerence tomography in an optic tract lesion: retinal nerve fiber layer changes. Neurology. 2016;87:2063–2064.
16. **Kanamori A**, Nakamura M, Yamada Y, Negi A. Spectral-domain optical coherence tomography detects optic atrophy due to optic tract syndrome. Graefes Arch Clin Exp Ophthalmol. 2013;251:591–595.
17. **Tieger MG**, Hedges TR III, Ho J, Erlich-Malona NK, Vuong LN, Athappilly GK, Mendoza-Santiesteban CE. Ganglion cell complex loss in chiasmal compression by brain tumors. J Neuroophthalmol. 2017;37:7–12.
18. **Kim JH**, Kim CY, Yang HK, Hwang JM. Unusual chiasmal visual field defects. Neurol Sci. 2013;34:2057–2060.
19. **Akashi A**, Kanamori A, Ueda K, Matsumoto Y, Yamada Y, Nakamura M. The detection of macular analysis by SD-OCT for optic chiasmal compression neuropathy and nasotemporal overlap. Invest Ophthalmol Vis Sci. 2014;55:4667–4672.